Catalysis Science & Technology

ROYAL SOCIETY OF CHEMISTRY

PAPER

View Article Online
View Journal | View Issue

Cite this: *Catal. Sci. Technol.*, 2025, **15**, 7190

Degradation and post-treatment reaction cascade of acetaminophen after electro-Fenton treatment on heterogeneous catalyst active sites

Fee Käufer *[ab] and Heike Kahlert [b]

Pharmaceuticals are not effectively removed from wastewater by traditional three step water purification methods, posing significant environmental and public health concerns. A heterogeneous electro-Fenton process was investigated as a promising treatment candidate and revealed a degradation mechanism with two stages for the common pharmaceutical acetaminophen. First, a traditional Fenton reaction occurs *in situ* at active sites of catalytic iron at the cathode. Hydroxyl radicals which are produced from hydrogen peroxide *via* the Fenton reaction lead to hydroxylation of acetaminophen. This primary degradation initialises a post-treatment reaction cascade leading to degradation *ex situ* over time. Without further energy input, continuous degradation of acetaminophen can be achieved. The main products of acetaminophen degradation caused by the Fenton reaction and other advanced oxidation processes (AOPs) as described in the literature are *p*-benzoquinone (BQ) and hydroquinone (HQ). Their occurrence is also likely in the described setup. Both can lead to formation of quinone anion radicals (QRs) by comproportionation. When QRs react with the weak oxidising agents present, hydrogen peroxide and oxygen, hydroxyl radicals and superoxide radicals are produced. These lead to further degradation processes towards the mineralisation of the remaining acetaminophen and its products. As BQ and HQ are degradation products of several aromatic pollutants, it is possible that the revealed mechanism is transferable to other pollutants and their degradation through the Fenton reaction. This emphasizes the importance of studying Fenton systems not only in batch or circular reactors, but also in continuous flow-through systems, allowing differentiation between effects caused by the two degradation stages.

Received 27th June 2025,
Accepted 27th September 2025

DOI: 10.1039/d5cy00784d

rsc.li/catalysis

1 Introduction

Pharmaceuticals are contaminants of emerging concern (CECs) because they have potential harmful effects on humans or the environment. Pharmaceuticals are of increasing importance in the context of water quality, especially as conventional wastewater treatment technologies are not designed to degrade them, making the challenge of effectively removing these pollutants from water sources increasingly critical.[1] In effluents from state-of-the-art wastewater treatment plants, pharmaceuticals are still present in concentrations in the range of ng L^{-1} to µg L^{-1}.[2] An extensive global study of surface waters detected pharmaceuticals in 134 of 137 sampling sites demonstrating the significance of the issue of pharmaceuticals in water systems.[3]

One promising treatment option for the removal of organic pollutants, including pharmaceuticals, from wastewater is the use of advanced oxidation processes (AOPs). These processes use the production of highly reactive oxidising agents, particularly hydroxyl radicals, which are known for their ability to effectively mineralise and break down complex organic compounds.[4] Among the various AOPs, the Fenton process is one of the most extensively studied. It utilises a reaction between hydrogen peroxide and iron(II) to generate hydroxyl radicals. The hydroxyl radicals produced in this process are highly reactive. They have a standard reduction potential $E^{\ominus}$ ($^{\bullet}OH/H_2O$ *vs.* SHE) of 2.8 V.[5] Therefore, they can initiate rapid oxidative degradation of organic compounds, ultimately leading to complete mineralisation. However, conventional homogeneous Fenton processes operate under acidic conditions, requiring a low pH environment, typically around 3. This can be problematic for practical applications, as acidification and subsequent neutralisation cause additional costs. In addition, iron pollution of treated water leads to further measures needed. To overcome these drawbacks, a heterogeneous system with the use of solid iron catalysts may be applied. This approach not only stabilises the catalyst, but also allows operation at a neutral pH, thereby improving the overall applicability of the

[a] *Leibniz Institute for Plasma Science and Technology, Felix-Hausdorff-Straße 2, 17489 Greifswald, Germany. E-mail: fee.kaeufer@inp-greifswald.de*
[b] *University of Greifswald, Felix-Hausdorff-Straße 4, 17489 Greifswald, Germany*

treatment process.[6] Moreover, the implementation of an electro-Fenton process presents a significant advancement in the field. In the electro-Fenton process, hydrogen peroxide is generated electrochemically through the two-electron oxygen reduction reaction, leading to *in situ* production of the oxidant. This not only enhances the efficiency of hydroxyl radical generation, but also avoids the logistical challenges associated with the storage, transportation, and handling of liquid hydrogen peroxide that are typical with traditional Fenton processes.[5]

Such electro-Fenton processes are usually operated in batch reactors. Here, the entire volume of the solution is treated simultaneously, and the reactants are thoroughly mixed with the untreated solution.[5] However, this approach has a significant limitation: it does not allow for differentiation of treatment processes on a temporal scale. As untreated solution is continuously mixed with the treated one, it becomes increasingly challenging to assess the distinct effects of the treatment *in situ* at the heterogeneous Fenton catalyst and its initiated reactions which occur post-treatment. To overcome this limitation, the present study employs a flow-through electro-Fenton system. In this approach, the flow originating from the cell's outlet is directed away from the original vessel containing untreated solution, thus creating a more controlled experimental environment. By maintaining this separation, the flow-through system enables a clearer assessment of how pollutants react over time at the catalyst not only *in situ* but also *ex situ*. This temporal analysis is critical to understanding the kinetics of pollutant removal and provides insight into how much degradation is caused by the energy-dependent electro-Fenton process and how much by a post-treatment reaction cascade. The possibility of such distinction is the novelty of the present study.

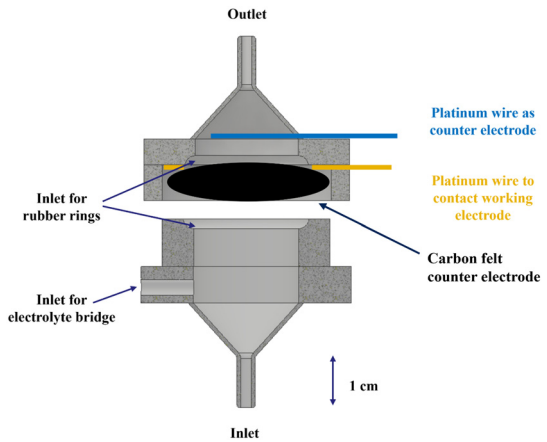

Fig. 1 Flow-through reaction cell with coated carbon felt as a working electrode, in contact circularly all around. The counter electrode is a platinum wire and a reference Ag/AgCl electrode is connected *via* an electrolyte bridge inserted through an inlet. Rubber rings are included for sealing.

2 Methods

2.1 System setup

A self-designed flow-through reaction cell was used for the investigated electro-Fenton setup (Fig. 1). It was designed using computer aided design (CAD) software (Autodesk Inventor Professional, Autodesk) and fabricated from resin (Clear, Formlabs) using a 3D printer (Form 2, Formlabs). To remove the residual liquid resin, the parts were placed in an isopropanol bath for 10 min in a Form Wash device (Formlabs). The material was cured for 15 min at 60 °C under 405 nm light in a Form Cure device (Formlabs).

Coated carbon felt H23C6 (Freudenberg) was applied as a working electrode and brought into contact with a platinum wire that encircled the carbon felt. It was coated with iron oxides *via* magnetron sputtering to provide a heterogeneous Fenton catalyst. Reactive sputtering was used for deposition by creating an atmosphere with a volumetric $Ar:O_2$ ratio of 5 : 8. At 6.5 Pa, 100 W was applied to an iron target. The process ran for 60 min. The catalytic material produced consisted of amorphous magnetite with a small proportion of low-crystalline hematite. Further details on the deposited iron oxide material and its characterisation can be found in a previous publication.[7]

The three-electrode setup was completed with a spiral of platinum wire as the counter electrode and Metrohm Ag/AgCl (saturated KCl(Honeywell, p.a.), E = 0.208 V *vs.* SHE) as a reference electrode which was connected *via* an electrolyte bridge to the reaction cell. The salt bridge contained an agar gel produced with saturated potassium chloride. Rubber rings were used above and below the working electrode to provide sealing.

2.2 System operation

The model pollutant acetaminophen (Sigma Aldrich, 98%) was added to a pH 6 50 mM sodium sulphate solution (Honeywell, ≥99%) to obtain an eluent containing 31.25 mg L^{-1} acetaminophen. It was pumped through the reaction cell using a peristaltic pump (IPC, Ismatec) at a flow rate of 1.5 mL min^{-1}. A potentiostatic approach was used. Once all electrodes were immersed in the eluent, a potential of −0.7 V was applied using a μAutolab Type II potentiostat (Metrohm) and controlled *via* Nova software (Metrohm Nova, version 2.0). Initially, the solution at the outlet was discarded to guarantee that the actual sample collected was homogeneous and that all of it interacted with the working electrode during application of the potential. The system was operated at room temperature with no observed changes during operation.

2.3 Sample analysis

The acetaminophen content of the collected samples was analysed by HPLC (1260 Infinity II LC System, Agilent Technologies) with a diode array detector and a Luna C18(2) 5 μm column (Phenomenex). The sample tray was

maintained at a temperature of 25 °C, and an injection of 50 μL from the sample was made for analysis. The mobile phase consisted of a mixture of methanol (≥99.8%, Fischer Chemical) and 0.1% phosphoric acid (obtained from 85% phosphoric acid, Merck), which was pumped through the system at a rate of 1 mL min^{-1}. Initially the composition was set at 10% methanol and 90% phosphoric acid. Over the first 14 min, this ratio was gradually adjusted to 100% methanol which was held for one minute. Afterwards, the mixture was slowly switched back to the starting ratio over three minutes and maintained for an additional two minutes. Meanwhile, the diode array detector monitored acetaminophen at 254 nm and collected the UV spectra for all emerging degradation products. The analysis of a sample by HPLC was conducted immediately following a run through the electro-Fenton reaction cell and further measurements followed continuously after for real-time analysis of the sample.

The degradation was calculated by taking the peak areas of acetaminophen from the chromatogram. The area for the initial untreated solution A_0 and the value for measured treated sample A_1 were related as follows:

$$\text{Degradation } [\%] = \left(1 - \frac{A_1}{A_0}\right) \cdot 100 \quad (1)$$

The presence of hydrogen peroxide was confirmed *via* the Ghormley triiodide method as described by Klassen *et al.*[8] It is based on the production of triiodide with hydrogen peroxide *via* the following two reactions:[8,9]

$$H_2O_2 + 2I^- + 2H^+ \rightleftarrows I_2 + H_2O \quad (2)$$

$$I_2 + I^- \rightleftarrows I_3^- \quad (3)$$

Triiodide strongly absorbs at 351 nm and therefore can be detected by UV-vis spectroscopy. Two solutions are required: one with 0.1 mol L^{-1} potassium hydrogen phthalate (Carl Roth) and a second one with a mixture of 0.4 mol L^{-1} potassium iodide (Carl Roth), 0.6 mol L^{-1} sodium hydroxide (Fisher Chemical), and 0.1 mmol L^{-1} ammonium molybdate tetrahydrate (Sigma Aldrich). Sodium hydroxide and potassium hydrogen phthalate were used to buffer the solution. Added ammonium molybdate catalyses the reaction of potassium iodide with hydrogen peroxide. A total of 750 μL of each solution was added to a cuvette (UV-Cuvette Marco, Brand), which contained 500 μL of the sample and 1000 μL of deionised water. After a 10 min reaction period, a UV-vis photometer (SPECORD 50, Analytik Jena AG) measured the spectrum from 200 nm to 500 nm, with a peak at 351 nm.

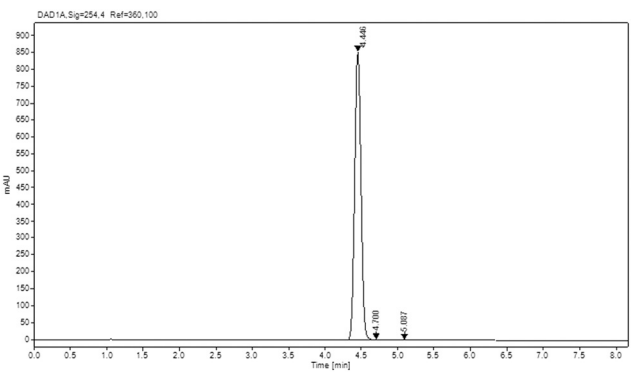

Fig. 2 Initial chromatogram recorded for the acetaminophen solution.

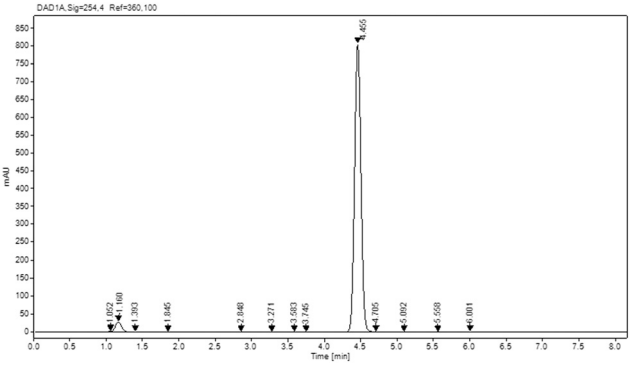

Fig. 3 Chromatogram of the acetaminophen solution treated by the described heterogeneous electro-Fenton system recorded at t = 0 min after treatment.

3 Results and discussion

3.1 Acetaminophen degradation

With the described HPLC procedure, the as-prepared acetaminophen solution's chromatogram showed a peak at a retention time of 4.45 min (Fig. 2). Immediately after treatment of the acetaminophen solution by the described heterogeneous electro-Fenton system, an initial degradation of 10.5(±1.6)% was observed as calculated by eqn (1). It should be noted that this immediate measurement is set as t = 0 even though approximately 5 min passed between sample extraction and beginning of the HPLC run. This time can be considered marginally small compared to measurement times. Additional peaks appeared in the corresponding chromatogram at t = 0, which must be due to degradation

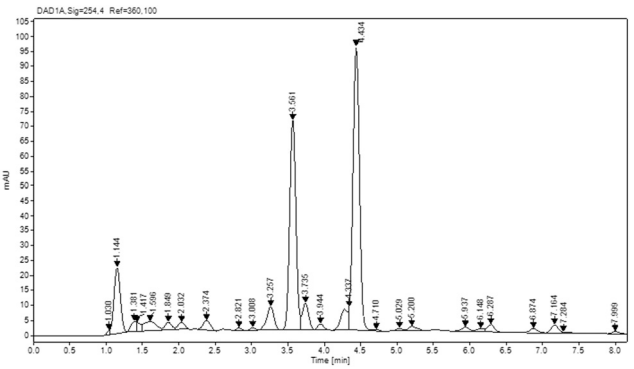

Fig. 4 Chromatogram of the acetaminophen solution treated by the described heterogeneous electro-Fenton system recorded at t = 1068 min after treatment.

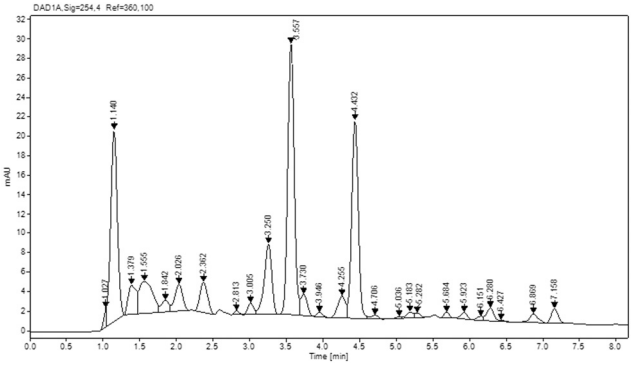

Fig. 5 Chromatogram of the acetaminophen solution treated by the described heterogeneous electro-Fenton system recorded at t = 1372 min after treatment.

products (Fig. 3). Measurements of the same sample at 1068 min and 1372 min after t = 0 showed a development in the observed chromatograms (Fig. 4 and 5). The peak of acetaminophen decreased further while others increased.

Following this observation, a detailed analysis of acetaminophen development over time after an initial treatment was performed. Keeping the sample at 25 °C and continuously analysing it using HPLC, an increase in degradation values was observed with each measurement. Plotting these values over time produces an S-shaped curve (Fig. 6). Its progression can be divided into three phases. Up to 100 min, during phase one a slight increase in acetaminophen degradation is detected. After this, the change in degradation increases dramatically and leads to an almost exponential progression in phase two. A plateau is reached in phase three. After about 12.5 h, the final degradation is 99.6% for repetition I, 99.7% for repetition II and 97.7% for repetition III. This suggests that only a small part of the degradation takes place *in situ* on the catalyst. The majority takes place *ex situ* as a result of a post-treatment reaction cascade.

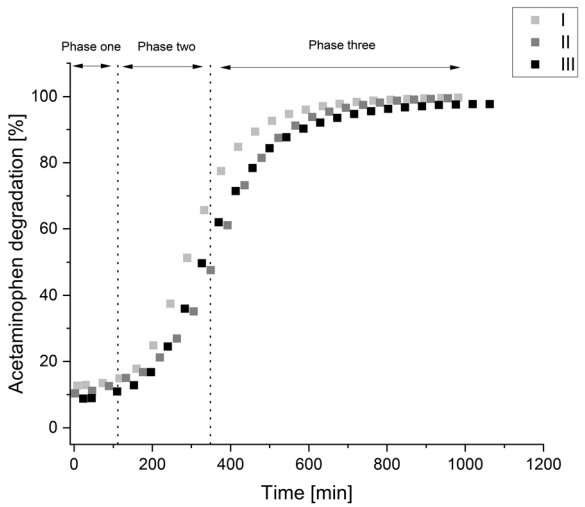

Fig. 6 Change in detected acetaminophen degradation over time for three samples which were treated by the electro-Fenton process and continuously kept at 25 °C for measurement by HPLC.

3.2 Mechanism for the reaction Cascade

This observed cascade must be driven by emerging degradation products. Various studies in batch reactors have detected similar products of acetaminophen from the reaction with hydroxyl radicals.[10–12] Vogna *et al.*[13] were the first to describe a detailed reaction pathway of acetaminophen treated by an AOP. The initial step in the degradation sequence always involves hydroxylation, which can occur at the *ortho*, *meta*, or *para* positions of the aromatic ring. However, investigations suggest that hydroxylation mainly takes place at *ortho*- and *para*-positions. During the operation of an electro-Fenton process, benzoquinone (BQ) has been identified as the primary degradation product.[14,15] BQ can result from hydroxylation at all positions on the aromatic ring. Only direct substitution at the *para*-position yields hydroquinone (HQ) instead of BQ (Fig. 7, path A). Both BQ and HQ are formed simultaneously along with acetamide, which is ultimately degraded to ammonium and small amounts of nitrate. Additional products identified in degradation of acetaminophen are 2-hydroxy-4-(*N*-acetyl) aminophenol (HAP), benzoic acid, and benzaldehyde. HAP is produced through hydroxylation at the *ortho*-position (Fig. 7, path B), while benzoic acid and benzaldehyde are derived from transformations of both HQ and BQ (Fig. 7).

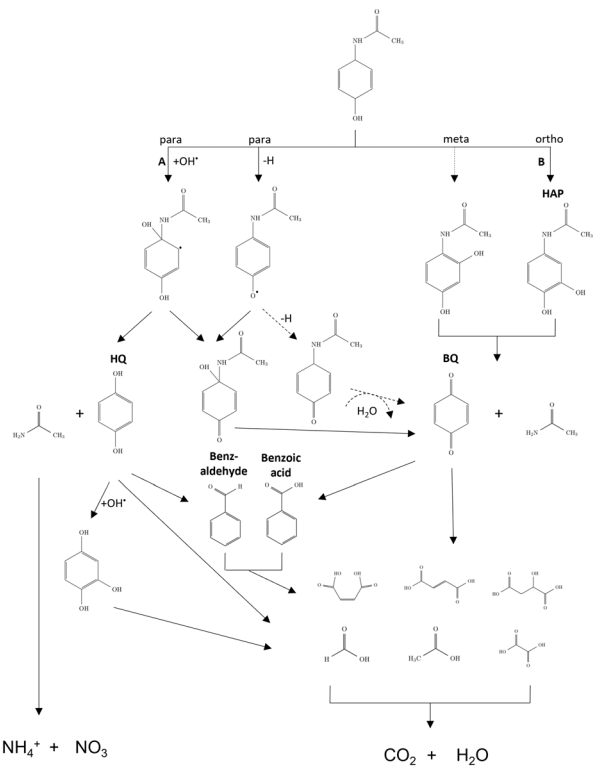

Fig. 7 Degradation pathway for acetaminophen as suggested in the literature.

Furthermore, aromatic ring cleavage facilitated by hydroxyl radicals is a viable mechanism, enabling the degradation of aromatic compounds into various carboxylic acids, including oxalic, maleic, oxamic, formic, acetic, and fumaric acids through AOPs. The subsequent oxidative processes ultimately convert these compounds into water and carbon dioxide completing full mineralisation of acetaminophen.[15]

None of the mentioned degradation products of acetaminophen seem to be suitable to initiate a post-treatment reaction cascade that explains the observed continuous *ex situ* degradation. Oxidising agents must be involved, which are neglected in the described pathway.

Within this study, effluent samples of the applied Fenton system contain at least two initial oxidising agents. For one, hydrogen peroxide is present in samples when not all of it reacts at catalytically active sites in a Fenton reaction. This was proven by detecting hydrogen peroxide photometrically in samples *via* the Ghormley triiodide method as described by Klassen *et al.*[8] The other oxidising agents present in the samples are oxygen molecules, which did not undergo the two-electron oxygen reduction reaction (ORR). Hydrogen peroxide is considered a weak oxidising agent, having a standard reduction potential $E^{\ominus}$ (H_2O_2/H_2O *vs.* SHE) of 1.763 V. As a result, it can only oxidise specific organic compounds, such as aldehydes and formic acid.[5,16] In comparison, molecular oxygen has an even lower standard reduction potential $E^{\ominus}$ (O_2/H_2O *vs.* SHE) of 0.804 V[17] (Fig. 8). Therefore, while both oxygen and hydrogen peroxide may contribute to the degradation of the final organic products resulting from acetaminophen toward complete mineralisation, the persistent degradation of acetaminophen cannot be solely attributed to direct oxidation by hydrogen peroxide or oxygen. This was confirmed by adding hydrogen peroxide to the acetaminophen solution and monitoring its amount. Over 10 h, a variation in acetaminophen concentration of only 0.32(±0.10)% was observed.

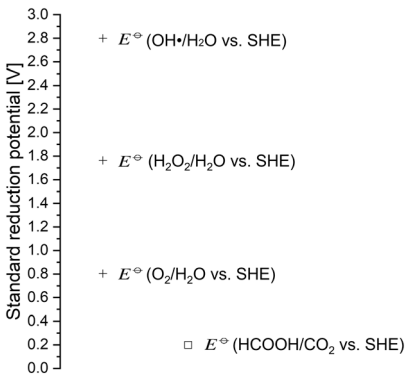

Fig. 8 Comparison of standard reduction potentials of the present oxidising agents (molecular oxygen, hydrogen peroxide and hydroxyl radicals) (+) with standard reduction potentials of certain organic compounds (□).

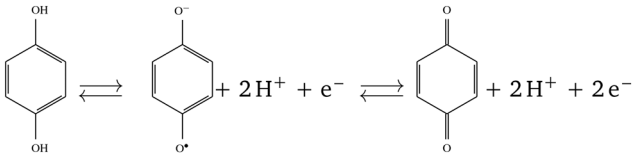

Fig. 9 Quinone anion radicals (QRs) as a redox intermediate of hydroquinone (HQ) and *p*-benzoquinone (BQ).

The post-treatment reaction cascade is likely driven by more reactive oxidising agents, most probably in the form of free radicals. One possible candidate is quinone anion radicals (QRs), which can be derived from the primary degradation products BQ and HQ. They can result from two different mechanisms. They are intermediates in the redox chemistry of BQ and HQ (Fig. 9).[18] During oxidation, HQ releases electrons, leading to the formation of QRs. This reaction is initiated by oxidising agents. Both molecular oxygen and hydrogen peroxide can act as such oxidising agents and lead to the formation of QRs by oxidation of HQ.[19,20] The other mechanism is the comproportionation of BQ and HQ, which leads to QRs (Fig. 10).[21] In this case, the occurrence of QRs depends on a reaction equilibrium between comproportionation and disproportionation (Fig. 10).

QRs, which can be generated by two distinct mechanisms, are highly reactive intermediates that are capable for further reactions. These radicals have the ability to activate both hydrogen peroxide and molecular oxygen, and convert them into highly reactive oxygen radicals.[22] In a so-called organic Fenton reaction, QRs facilitate the generation of reactive hydroxyl radicals in the presence of hydrogen peroxide (reaction (4)). When QRs interact with molecular oxygen, they form superoxide anion radicals (reaction (5)).[23] Due to their reactivity, QRs are gradually consumed in these processes, which shifts the equilibrium of comproportionation and disproportionation reactions toward the formation of additional QRs. This results in a steady production of QRs which provide a source of highly reactive radical species *via* reactions (4) and (5). These reactive species can interact not only with acetaminophen, but also with its degradation products, which initiates a post-treatment reaction cascade. Therefore, the formation of QRs from the primary degradation products BQ and HQ contributes to an ongoing degradation process that continues even after acetaminophen has left the electro-Fenton system and its reaction sites at the cathode. This process is limited by the availability of

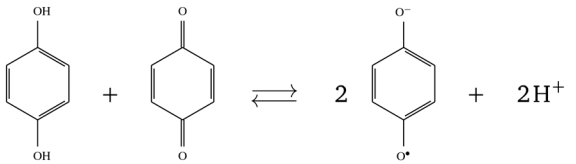

Fig. 10 Hydroquinone (HQ) and *p*-benzoquinone (BQ) comproportionate to quinone anion radicals (QRs).

hydrogen peroxide, molecular oxygen, and HQ. Nevertheless, the hydroxylation of acetaminophen at the *para*-position can continue to form HQ for some time while QRs react with hydrogen peroxide, maintaining the cycle of oxidation and degradation within the system.

$$QR + H_2O_2 + H^+ \rightleftarrows BQ + OH^- + H_2O + OH^{\bullet} \quad (4)$$

$$QR + O_2 \rightleftarrows BQ + O_2^{-\bullet} \quad (5)$$

3.3 Degradation products

Previous studies have detailed the degradation pathway of acetaminophen in batch experiments, so it is important to compare whether the post-treatment reaction cascade leads to any variation of it.

Analysing samples using HPLC enables the detection of degradation products. The instrumentation used in this study includes a UV detector that offers three approaches for identifying the detected degradation products. Firstly, analysing the progression of product concentrations in relation to the proposed degradation pathway can provide valuable insight into the reaction dynamics. In addition, UV spectra are recorded for each product as it elutes from the column, allowing direct comparison with known UV absorption bands and full spectra of expected substances. Finally, the retention time provides additional information about the polarity of the products. The HPLC column used in this analysis is a Luna C18(2) column, which operates in reversed-phase mode. The stationary phase is therefore non-polar. Consequently, polar substances have shorter retention times compared to non-polar substances when using this instrument. This combination of techniques enables assumptions about arising degradation products. For certain identification, a mass spectrometer would be preferable which was not available for the present study.

For the samples whose acetaminophen degradation is described in section 3.1, the occurring degradation products were investigated. These are illustrated below using a representative sample. A total of 23 degradation products were detected, which occur at different times after treatment with the electro-Fenton system. They each show different concentration trends. The main products observed which are discussed in more detail below, are named according to their retention time P1 to P6 (Table 1). Their relative changes are plotted by normalising the peak areas to the largest peak area detected, which was set to 1. This leads to graphs showing the progression over time of these products during the post-treatment reaction cascade. All other detected products are analogously named S1 to S17 (Table 1).

The main degradation product, called P4, has the largest peak areas and has a retention time of 3.58 min. It is detected in every measurement from the first to the last measurement. Its progression is particularly remarkable when the three phases of acetaminophen degradation are considered. In phase one, P4 increases linearly, while its concentration increases exponentially in phase two. In phase three, however, its amount decreases rapidly (Fig. 11, dark blue). Thus, the production of P4 coincides with the phases of acetaminophen degradation, except for its behaviour in phase three, where it does not reach saturation but is degraded, leading to its removal. P4 is most likely BQ, as it is recognised as the primary degradation product of acetaminophen.[14,15] The recorded UV spectrum shows clear absorption bands, with a significant band at around 248 nm (Fig. 12). The curve of the overall spectrum correlates well with that for BQ.[24,25] It is therefore assumed that P4 is BQ.

After P4, P5 has the second largest peak areas in chromatographic analysis. Its quantity profile is similar to that of BQ in phase two. Although P5 is present in the first phase, its quantity increases only slightly. In the third phase, P5 disappears almost completely (Fig. 11, light blue). The chromatogram shows P5 as a shoulder on the peak corresponding to BQ (P4), indicating the similar structure and polarity of the two compounds. It occurs at a retention time of 3.75 min.

Table 1 Retention times (RTs) for all 23 detected degradation products. Substances P1 to P6 are the main products which are discussed further within this article

RT [min]	1.05	**1.15**	1.61	**1.86**	**2.03**	2.25	2.37	2.84
Name	S1	**P1**	S2	**P2**	**P3**	S3	S4	S5
Candidate	—	**Acetamide**	—	—	—	—	—	—
RT [min]	3.01	3.27	**3.58**	**3.75**	3.96	4.28	**4.64**	5.04
Name	S6	S7	**P4**	**P5**	S8	S9	**P6**	S10
Candidate	—	—	**BQ**	**HQ**	—	—	**NAPQI**	—
RT [min]	5.19	5.23	5.97	6.15	6.29	6.87	7.16	
Name	S11	S12	S13	S14	S15	S16	S17	
Candidate	—	—	—	—	—	—	—	

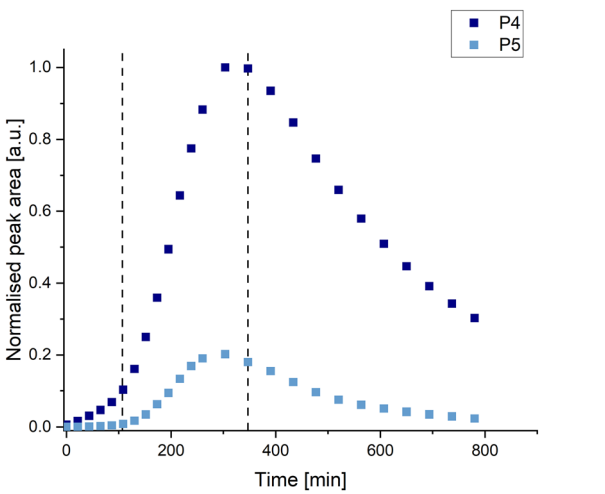

Fig. 11 Occurrence and progression over time of normalised peak areas of main degradation products P4 and P5 detected after treatment of the acetaminophen solution with the electro-Fenton process.

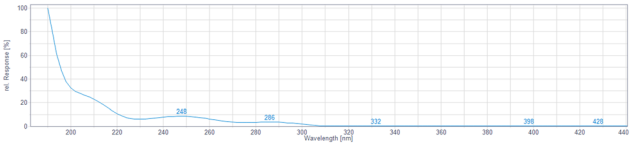

Fig. 12 UV spectrum recorded for P4.

The early detection of P5 in the initial measurement indicates that it is probably a primary degradation product. In addition to hydroxylation at the *ortho*-position, which leads to the formation of BQ, hydroxylation at the *para*-position is also possible, resulting in the generation of two short-lived radicals. These radicals can convert to BQ or HQ indirectly *via* pathway A (Fig. 7). As a result, similar trends in HQ and BQ concentrations can be expected. However, HQ is expected to be formed in lower amounts as fewer metabolic pathways are available for its production. The recorded UV spectrum for P5 shows an absorption band near 282 nm (Fig. 13). This band is known for HQ.[26] Based on these results, it is assumed that P5 is HQ.

Based on the considerations discussed in section 3.2, a more detailed analysis of the dynamics of BQ and HQ was performed. It is important to recognise that the observed concentration profiles of these compounds reflect only the final changes within the system. An increase in concentration, while indicative of production processes, may mask underlying removal mechanisms that occur at reduced rates. Similarly, a decrease in concentration does not exclude the possibility of simultaneous production of these compounds at lower rates.

During phase one, the degradation of acetaminophen shows only minimal changes (Fig. 6), and the concentrations of HQ remain relatively stable. In contrast, a more pronounced increase is observed for BQ (Fig. 11). This relationship illustrates the dependence between the degradation of acetaminophen and the formation of its degradation products. If acetaminophen is not degraded, no corresponding degradation products can be formed. In phase two, the concentrations of BQ and HQ reach values that must allow their comproportionation (Fig. 10), which leads to the formation of QRs. These QRs can react *via* reactions (4) and (5) to form new strong oxidising agents $OH^{\bullet}$ and $O_2^{-\bullet}$ in the sample. After the degradation of acetaminophen molecules caused by these radicals, additional BQ and HQ are produced, which can form more QRs through further comproportionation. This continuous production of BQ and HQ, coupled with the removal of QRs *via* reactions (4) and (5), shifts the equilibrium in favour of the comproportionation processes. This leads to an exponential decay of acetaminophen and simultaneously to an increase in the concentrations of BQ and HQ. The beginning of phase three marks an important turning point in the reaction dynamics. The concentrations of BQ and HQ begin to decrease, while the rate of acetaminophen degradation also slows down. As fewer acetaminophen molecules are present in the system, the likelihood of interactions producing these degradation products decreases, leading to a predominant breakdown of the existing degradation products. As a result, the direct production of the primary degradation products BQ and HQ by acetaminophen degradation decreases. At the same time, they continue to be involved in comproportionation reactions. HQ decreases during the entire third phase, and disappears almost completely at the end of this phase. This decrease is to be expected as HQ serves as a limiting reactant in the suggested post-treatment reaction cascade.

The two other degradation products that will be discussed in detail are P1 and P6. P1 is present from the beginning and is formed with increasing rate during phase two, and finally reaches a steady state in phase three (Fig. 14, orange). The very short retention time of 1.15 min indicates that P1 is very polar. In addition, the recorded UV spectrum for P1 does not exhibit any absorption bands (Fig. 15).

Acetamide is a degradation product formed from each molecule of BQ and HQ. This indicates that acetamide must also be present from the beginning, with its concentration increasing during phase two. According to the literature, the UV spectrum of acetamide shows no absorption bands.[27]

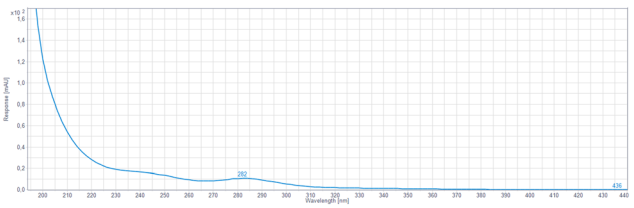

Fig. 13 UV spectrum recorded for P5.

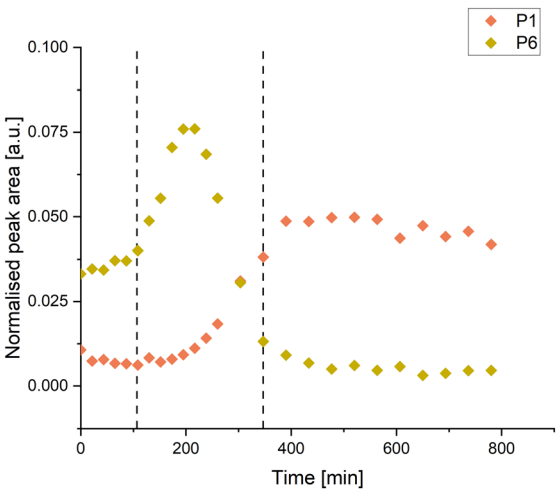

Fig. 14 Occurrence and progression over time of normalised peak areas of degradation products P1 and P6 occurring right from the beginning as detected after treatment of the acetaminophen solution with the electro-Fenton process.

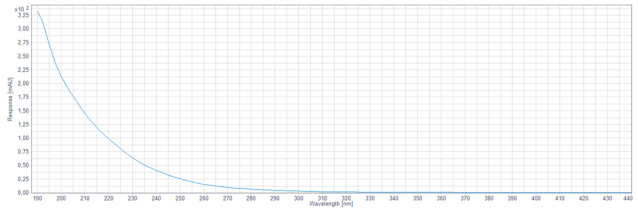

Fig. 15 UV spectrum recorded for P1.

Furthermore, since acetamide is a polar molecule,[28] its short retention time fits well with P1. Therefore, it is assumed that P1 is acetamide.

P6 has unique characteristics, as it is detected not only in the initial measurements, but also in the acetaminophen solution prior to treatment with the electro-Fenton process. The concentration of P6 rises gradually in phase one, increases sharply in phase two, and then decreases rapidly. In phase three, only trace amounts of P6 remain (Fig. 14, gold). In the chromatograms, P6 appears as a peak shoulder at a retention time of 4.64 min next to acetaminophen. This close retention time suggests that P6 and acetaminophen are structurally similar and have comparable polarities. The UV spectrum further supports this, as it shows an absorption band at 244 nm for P6 (Fig. 16), which is also characteristic of acetaminophen.[29]

The presence of P6 in the untreated acetaminophen solution indicates that this compound is not only a product of acetaminophen oxidation by the Fenton reaction. One possible explanation is that P6 can also be formed in the presence of weak oxidising agents such as oxygen. A likely candidate for P6 is therefore *N*-acetyl-*p*-benzoquinone imine (NAPQI). It can be produced directly through the oxidation of acetaminophen by various oxidising agents.[30] Due to the structural similarity between NAPQI and acetaminophen, this also explains their analogous retention times and UV spectra. It is therefore reasonable to assume that P6 is NAPQI.

The study of the progression shows that the degradation of acetaminophen leads to a lower NAPQI formation, while further oxidation processes seem to degrade NAPQI. This is a positive indication for the proposed electro-Fenton system and is essential as NAPQI is a very toxic compound.[31] For a reasonable and useful degradation process, it is necessary that the proposed electro-Fenton system shows effective degradation not only of acetaminophen, but also of its degradation products, especially the toxic ones. This is the case with the proposed system, as shown by the degradation of NAPQI.

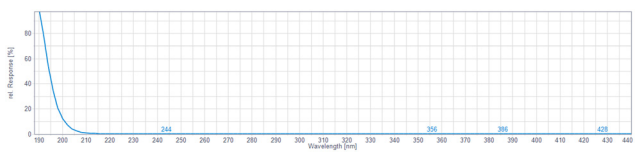

Fig. 16 UV spectrum recorded for P6.

Products P2 and P3, with retention times of 1.86 min and 2.03 min, respectively, serve as representative examples of other products detected in the study.

P2 is observed during phase one, and its concentration increases throughout phase two before subsequently decreasing in phase three (Fig. 17, light green). This progression suggests that there is successful breakdown of degradation products as part of the post-treatment reaction cascade, highlighting the dynamic nature of the chemical reactions occurring within the system.

In contrast, P3 only appears at the end of phase two (Fig. 17, dark green), which indicates that this is a product that is further down the degradation pathway. The appearance of P3 is a promising indicator that not only the oxidation of acetaminophen and its primary products takes place, but also the degradation of secondary and tertiary products. The concentrations of P3 remain stable at the end of the observation period, suggesting that the post-treatment reaction cascade may be approaching stagnation. This stagnation could be due to the insufficient availability of key reactants, such as HQ, hydrogen peroxide, or molecular oxygen, which are essential for maintaining the ongoing degradation processes.

If no hydrogen peroxide or molecular oxygen remains in the sample, reactions (4) and (5) can no longer take place. On the one hand, this not only shifts the equilibrium of comproportionation and dissociation as no QRs are removed, but also stops the production of new strong oxidising agents $OH^{\bullet}$ and $O_2^{-\bullet}$. At the same time, the lack of HQ shifts the equilibrium towards dissociation and stops the mechanism that drives the post-treatment reaction cascade.

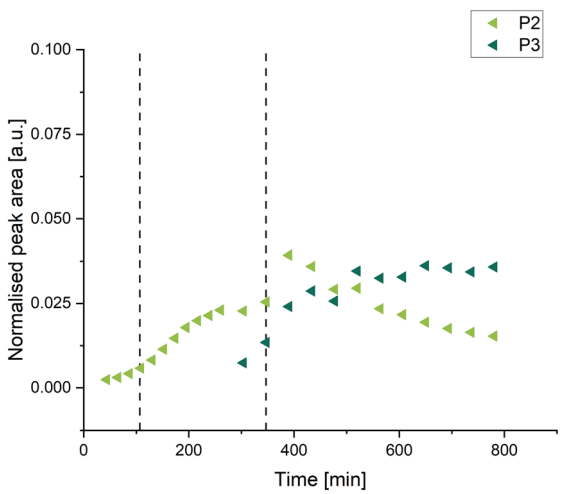

Fig. 17 Occurrence and progression over time of normalised peak areas of secondary and tertiary degradation products P2 and P3 as detected after treatment of the acetaminophen solution with the electro-Fenton process.

Conclusions

The continuous analysis of samples treated in a flow-through electro-Fenton system showed that the time elapsed between sample production and its measurement by HPLC has a significant influence on the degradation observed. This suggests that the processes at the catalyst can be regarded as an initiation step for a subsequent reaction cascade. This behaviour is explained by the formation of radicals, and thus a post-treatment reaction cascade involving BQ, HQ, QRs, hydrogen peroxide, and molecular oxygen. To the best of our knowledge, the occurrence of such a post-treatment reaction cascade and its contribution to degradation in Fenton systems have not been previously described in the literature.

This finding provides new insights into publications studying electro-Fenton systems, especially since most studies reported in the literature investigate an electro-Fenton system using batch reactors.[32] In these, the effects of time cannot be separated as the effluent is mixed with the influent. Hence, degradation by secondary radicals is neglected and attributed to the Fenton reaction in most studies, although a large part of the observed degradation is caused by a post-treatment reaction cascade independent of the Fenton reaction sites. This indicates an alternative degradation process that requires more time but less energy input, as only an initial Fenton process may be required. If faster decontamination is required, adding an additional treatment step within the same system could introduce additional strong oxidising species, thereby accelerating overall degradation.

In addition, other organic pollutants that contain an aromatic ring also have BQ and HQ as degradation products.[33–36] This leads to the assumption that the post-treatment reaction cascade described is also relevant for pollutants other than acetaminophen. In further investigations, an application of the described flow-through system with different substances as well as their mixtures would be interesting. Also, future measurements by HPLC-MS would add to the described results to allow distinct identification of all arising products and oxidising species. Further suggested experimental series include the systematic addition of radical scavengers to clarify the role of radical intermediates in the degradation pathways, as well as independent total organic carbon (TOC) analysis to quantify the reaction cascade's capacity for complete mineralisation.

Conflicts of interest

There are no conflicts to declare.

Data availability

Data will be made available upon request.

Acknowledgements

This research was funded by the Friedrich Ebert Foundation.

References

1 T. Nawaz and S. Sengupta, *Advances in water purification techniques*, Elsevier, Amsterdam, Netherlands, 2019, pp. 67–114.
2 H. B. Quesada, A. T. A. Baptista, L. F. Cusioli, D. Seibert, C. de Oliveira Bezerra and R. Bergamasco, *Chemosphere*, 2019, **222**, 766–780.
3 J. L. Wilkinson, A. B. A. Boxall, D. W. Kolpin, K. M. Y. Leung, R. W. S. Lai, C. Galbán-Malagón, A. D. Adell, J. Mondon, M. Metian, R. A. Marchant, A. Bouzas-Monroy, A. Cuni-Sanchez, A. Coors, P. Carriquiriborde, M. Rojo, C. Gordon, M. Cara, M. Moermond, T. Luarte, V. Petrosyan, Y. Perikhanyan, C. S. Mahon, C. J. McGurk, T. Hofmann, T. Kormoker, V. Iniguez, J. Guzman-Otazo, J. L. Tavares, F. Gildasio De Figueiredo, M. T. P. Razzolini, V. Dougnon, G. Gbaguidi, O. Traoré, J. M. Blais, L. E. Kimpe, M. Wong, D. Wong, R. Ntchantcho, J. Pizarro, G.-G. Ying, C.-E. Chen, M. Páez, J. Martínez-Lara, J.-P. Otamonga, J. Poté, S. A. Ifo, P. Wilson, S. Echeverría-Sáenz, N. Udikovic-Kolic, M. Milakovic, D. Fatta-Kassinos, L. Ioannou-Ttofa, V. Belušová, J. Vymazal, M. Cárdenas-Bustamante, B. A. Kassa, J. Garric, A. Chaumot, P. Gibba, I. Kunchulia, S. Seidensticker, G. Lyberatos, H. P. Halldórsson, M. Melling, T. Shashidhar, M. Lamba, A. Nastiti, A. Supriatin, N. Pourang, A. Abedini, O. Abdullah, S. S. Gharbia, F. Pilla, B. Chefetz, T. Topaz, K. M. Yao, B. Aubakirova, R. Beisenova, L. Olaka, J. K. Mulu, P. Chatanga, V. Ntuli, N. T. Blama, S. Sherif, A. Z. Aris, L. J. Looi, M. Niang, S. T. Traore, R. Oldenkamp, O. Ogunbanwo, M. Ashfaq, M. Iqbal, Z. Abdeen, A. O'Dea, J. M. Morales-Saldaña, M. Custodio, H. de La Cruz, I. Navarrete, F. Carvalho, A. B. Gogra, B. M. Koroma, V. Cerkvenik-Flajs, M. Gombač, M. Thwala, K. Choi, H. Kang, J. L. C. Ladu, A. Rico, P. Amerasinghe, A. Sobek, G. Horlitz, A. K. Zenker, A. C. King, J.-J. Jiang, R. Kariuki, M. Tumbo, U. Tezel, T. T. Onay, J. B. Lejju, Y. Vystavna, Y. Vergeles, H. Heinzen, A. Pérez-Parada, D. B. Sims, M. Figy, D. Good and C. Teta, *Proc. Natl. Acad. Sci. U. S. A.*, 2022, **119**, 1–10.
4 D. B. Miklos, C. Remy, M. Jekel, K. G. Linden, J. E. Drewes and U. Hübner, *Water Res.*, 2018, **139**, 118–131.
5 I. Sirés and E. Brillas, *Electro-Fenton Process*, Springer Singapore, Singapore, 2018, pp. 1–28.
6 P. V. Nidheesh, H. Olvera-Vargas, N. Oturan and M. A. Oturan, *Electro-Fenton Process*, Springer Singapore, Singapore, 2018.
7 F. Käufer, A. Quade, A. Kruth and H. Kahlert, *Nanomaterials*, 2024, **14**, 252.
8 N. V. Klassen, D. Marchington and H. C. McGowan, *Anal. Chem.*, 1994, **66**, 2921–2925.
9 A. O. Allen, C. J. Hochanadel, J. A. Ghormley and T. W. Davis, *J. Phys. Chem.*, 1952, **56**, 575–586.
10 S. Feng, X. Zhang and Y. Liu, *Water Res.*, 2015, **86**, 35–45.
11 M. D. G. de Luna, M. L. Veciana, C.-C. Su and M.-C. Lu, *J. Hazard. Mater.*, 2012, **217–218**, 200–207.
12 E. Leyva, E. Moctezuma, K. M. Baines, S. Noriega and E. Zarazua, *Curr. Org. Chem.*, 2018, **22**, 2–17.

13 D. Vogna, R. Marotta, A. Napolitano and M. D'Ischia, *J. Org. Chem.*, 2002, **67**, 6143–6151.
14 H. Olvera-Vargas, J.-C. Rouch, C. Coetsier, M. Cretin and C. Causserand, *Sep. Purif. Technol.*, 2018, **203**, 143–151.
15 T. X. H. Le, T. van Nguyen, Z. Amadou Yacouba, L. Zoungrana, F. Avril, D. L. Nguyen, E. Petit, J. Mendret, V. Bonniol, M. Bechelany, S. Lacour, G. Lesage and M. Cretin, *Chemosphere*, 2017, **172**, 1–9.
16 M. Ramdin, A. R. Morrison, M. De Groen, R. Van Haperen, R. De Kler, E. Irtem, A. T. Laitinen, L. J. Van Den Broeke, T. Breugelmans and J. M. Trusler, *et al.*, *Ind. Eng. Chem. Res.*, 2019, **58**, 22718–22740.
17 W. H. Koppenol, D. M. Stanbury and P. L. Bounds, *Free Radical Biol. Med.*, 2010, **49**, 317–322.
18 G. E. Adams and B. D. Michael, *Trans. Faraday Soc.*, 1967, **63**, 1171.
19 V. A. Roginsky, L. M. Pisarenko, W. Bors and C. Michel, *J. Chem. Soc., Perkin Trans. 2*, 1999, 871–876.
20 A. Jakubiak-Marcinkowska, M. Legan and J. Jezierska, *J. Polym. Res.*, 2013, **20**, 317.
21 P. Sanchez-Cruz, A. Santos, S. Diaz and A. E. Alegría, *Chem. Res. Toxicol.*, 2014, **27**, 1380–1386.
22 G. Fang, J. Gao, D. D. Dionysiou, C. Liu and D. Zhou, *Environ. Sci. Technol.*, 2013, **47**, 4605–4611.
23 W. H. Koppenol and J. Butler, *Adv. Free Radical Biol. Med.*, 1985, **1**, 91–131.
24 F. Samiee, F. N. Pedron, D. A. Estrin and L. Trevani, *J. Phys. Chem. B*, 2016, **120**, 10547–10552.
25 N. I. of Standards and Technology, *NIST Chemistry WebBook: Specific Spectrum Identifier*, 2023, **https://webbook.nist.gov/cgi/cbook.cgi?ID=106-51-4**, accessed: 2025-03-04.
26 Sirajuddin, M. I. Bhanger, A. Niaz, A. Shah and A. Rauf, *Talanta*, 2007, **72**, 546–553.
27 X.-R. Lei, C. Gong, Y.-L. Zhang and X. Xu, *Chromatographia*, 2016, **79**, 1257–1262.
28 C. Chipot, *J. Comput. Chem.*, 2003, **24**, 409–415.
29 B. Manu, S. Mahamood, V. Hari and S. Surathkal, *Int. J. Res. Chem. Environ.*, 2011, **1**, 157–164.
30 M. Bedner and W. A. MacCrehan, *Environ. Sci. Technol.*, 2006, **40**, 516–522.
31 M. Moore, H. Thor, G. Moore, S. Nelson, P. Moldéus and S. Orrenius, *J. Biol. Chem.*, 1985, **260**, 13035–13040.
32 M. Panizza and O. Scialdone, *Electro-Fenton Process*, Springer Singapore, Singapore, 2018, pp. 205–240.
33 Y. Li and H. Cheng, *Chem. Eng. J.*, 2022, **449**, 137812.
34 A. Pinedo, M. López, E. Leyva, B. Zermeño, B. Serrano and E. Moctezuma, *Int. J. Chem. React. Eng.*, 2016, **14**, 809–820.
35 X. Li, Y. Wang, S. Yuan, Z. Li, B. Wang, J. Huang, S. Deng and G. Yu, *Water Res.*, 2014, **63**, 81–93.
36 C. Lara-Pérez, E. Leyva, B. Zermeño, I. Osorio, C. Montalvo and E. Moctezuma, *Environ. Earth Sci.*, 2020, **79**, 1–13.